

Parameters in a Class of Leptophilic Dark Matter Models from PAMELA, ATIC and FERMI

^{1,2}Xiao-Jun Bi, ^{1,3}Xiao-Gang He, ²Qiang Yuan

¹*Center for High Energy Physics, Peking University, Beijing 100871*

²*Laboratory of Particle Astrophysics, Institute of High Energy Physics, Chinese Academy of Sciences, Beijing 100049*

³*Department of Physics, Center for Theoretical Sciences, and LeCospa Center, National Taiwan University, Taipei*

In this work we study a class of leptophilic dark matter models, where the dark matter interacts with the standard model particles via the $U(1)_{L_i-L_j}$ gauge boson, to explain the e^\pm excess in cosmic rays observed by ATIC and PAMELA experiments, and more recently by Fermi experiment. There are three types of $U(1)_{L_i-L_j}$ models: a) $U(1)_{L_e-L_\mu}$, b) $U(1)_{L_e-L_\tau}$, and c) $U(1)_{L_e-L_\tau}$. Although ATIC or Fermi data is consistent with PAMELA data separately, ATIC and Fermi data do not agree with each other. We therefore aim to identify which of the three models can explain which data set better. We find that models a) and b) can give correct dark matter relic density and explain the ATIC and PAMELA data simultaneously recur to the Breit-Wigner enhancement. Whereas model c) with a larger Z' mass can explain Fermi and PAMELA data simultaneously. In all cases the model parameters are restricted to narrow regions. Future improved data will decide which set of data are correct and also help to decide the correct dark matter model.

PACS numbers: 98.80.Cq 11.15.Tk 11.25.Hf 14.80.-j

I. INTRODUCTION

Recently, the ATIC and PPB-BETS balloon experiments have observed excess in the $e^+ + e^-$ energy spectrum between 300 and 800 GeV [1, 2]. The PAMELA collaboration has also reported excesses in the positron fraction from 10 to ~ 100 GeV, but shown no excess for the antiproton data [3, 4] compared with the prediction in the cosmic ray physics. These results are compatible with the previous HEAT and AMS01 experiments (e.g., [5, 6, 7]) with

higher precision. Newly published result from Fermi also shows an excess at the $e^+ + e^-$ energy spectrum above the background of the conventional cosmic ray model. However, it shows a softer spectrum than ATIC [8]. The excesses may be explained by astrophysical processes, for instance the nearby pulsars [9, 10, 11] or photon-cosmic ray interactions [12], or due to annihilation or decay of dark matter (DM) particles in our Galactic neighbourhood predominately into leptons (e.g., [13, 14, 15, 16, 17, 18, 19]). Similar explanation can also account for the excess observed at Fermi by assuming a softer injection electron spectrum from these sources [20]. PAMELA indicate that the dark matter is hadrophobic or leptophilic[18]. In this work we show that gauged $U(1)_{L_i-L_j}$ models proposed some time ago[21] in searching for simple Z' can naturally explain the excess in electron/positron spectrum through the DM annihilation mechanism. Here L_i and L_j are one of the three family lepton numbers with $i \neq j$.

In constructing dark matter models, one should note that although ATIC or Fermi data is consistent with PAMELA data separately, ATIC and Fermi data do not agree with each other. Improved data are needed to decide which ones are correct and to distinguish different dark matter models. In the models we are considering, there are three different ways to gauge the lepton number differences: a) $U(1)_{L_e-L_\mu}$, b) $U(1)_{L_e-L_\tau}$, and c) $U(1)_{L_e-L_\tau}$. Each of them has different features. Our aim in this work is to identify which of the three models can explain which data set better.

The Z' in the gauged $U(1)_{L_i-L_j}$ is leptophilic which only interacts with standard model (SM) leptons. If the Z' also interacts with DM[14, 19], it will be the main mediator for DM annihilation with final product dominated by leptons offering possible explanation to electron/positron excess without anti-proton excess at PAMELA data.

Another requirement for DM annihilation to account for the positron excess is that the annihilation rate $\langle\sigma v\rangle$ determining the electron/positron spectrum should be much larger than that determined from the usual thermal DM relic density. The enhancement factor, usually referred as the boost factor, is in the range of $100 \sim 1000$. Several mechanisms have been proposed to produce a large boost factor, including the DM substructures, DM nonthermal production mechanism [22], the Sommerfeld effect [14, 15, 16, 23] and the Breit-Wigner resonance enhancement effect [24]. The detailed calculation based on the N-body simulation shows that the boost factor from DM substructures is generally less than ~ 10 [25, 26]. In order for the Sommerfeld effect to be effective, the mediating particle needs

to be very light to allow long range interaction between DM particles. This mechanism in our case will result in a light Z' boson. However, there are very tight constraints on the coupling constant for such light Z' . Instead the Breit-Wigner resonance enhancement mechanism works very well in our model if the Z' mass is about two times of the dark matter mass. From the relic density and ATIC, Fermi and PAMELA data we can also constrain the $U(1)_{L_i-L_j}$ charge of DM. There is no need to have very different $U(1)_{L_i-L_j}$ charges of DM and SM leptons as in [18]. Further, the determined $U(1)_{L_i-L_j}$ gauge coupling strength is consistent with all constraints from LEP, $(g-2)_\mu$ and other data.

The ATIC data also show a sharp falling at about 600 GeV in the electron/positron energy spectrum. We find such a feature needs substantial electron component as the DM annihilation products with the electron and positron pairs have a fixed energy from DM annihilation. Additional electron/positron energy spectrum with lower energy from secondary decays will then help to enhance positron with lower energies. We find that the gauged $U(1)_{L_e-L_\mu}$ (model a)) and $U(1)_{L_e-L_\tau}$ (model b)) can give excellent fit to the ATIC data while the $U(1)_{L_\mu-L_\tau}$ can not. On the contrary, Fermi shows a much softer electron spectrum, which does not favor the initial electron component. We find that the gauged $U(1)_{L_\mu-L_\tau}$ (model c)) gives an excellent fit to the Fermi, PAMELA and HESS data.

The paper is organized as following: in Sec. II we give a brief introduction of the model. In Sec. III we introduce the Breit-Wigner mechanism and the numerical results of relic density and boost factor in our model. Then we show the electron/positron spectrum of our model in Sec. IV. Finally we give discussions and conclusions in Sec. V.

II. THE MODEL

One of the following global symmetries in the SM can be gauged without gauge anomalies[21]

$$L_e - L_\mu, \quad L_e - L_\tau, \quad L_\mu - L_\tau .$$

The gauge boson Z' resulting from one of the above models has the desired leptophilic couplings. At the tree-level the Z' only couples to one of the pairs e and μ , e and τ , and μ and τ . We will use Y' to indicate the quantum numbers for one of the above three possibilities, $Y' = L_i - L_j$. If the Z' in one of these models is the messenger mediating dark matter annihilation, the resulting final states are mainly leptonic states which can lead

to electron/positron excess observed in cosmic rays. It is then desirable to have the Z' to couple to dark matter[14, 19]. We therefore introduce a new vector-like fermion ψ with a non-trivial Y' number a . The reason for the dark matter being vector-like is to make sure that the theory does not have gauge anomaly required for self consistency. The Z' boson can develop a finite mass from spontaneous $U(1)_{L_i-L_j}$ symmetry breaking of a scalar S with a non-trivial charge $Y' = b$. With the new particles Z' , S and ψ in the model, addition term L_{new} have to be added to the Lagrangian beside the SM one L_{SM} with

$$L_{new} = -\frac{1}{4}Z'^{\mu\nu}Z'_{\mu\nu} + \sum_l \bar{l}\gamma^\mu(-g'Y'_l Z'_\mu)l + \bar{\psi}[\gamma^\mu(i\partial_\mu - ag'Z'_\mu) - m_\psi]\psi + (D_\mu S)^\dagger(D^\mu S) + \mu_S^2 S^\dagger S + \lambda_S(S^\dagger S)^2 + \lambda_{SH}(S^\dagger S)H^\dagger H, \quad (1)$$

where l is summed over the SM leptons. H is the usual SM Higgs doublet.

The Z' coupling to fermions are given by

$$L = -g'(a\bar{\psi}\gamma^\mu\psi + \bar{l}_i\gamma^\mu l_i - \bar{l}_j\gamma^\mu l_j + \bar{\nu}_i\gamma^\mu L\nu_i - \bar{\nu}_j\gamma^\mu L\nu_j)Z'_\mu. \quad (2)$$

Note that the Z' coupling to leptons are flavor diagonal. There is no tree level flavor changing neutral current induced by Z' .

After S and H develop non-vanishing vacuum expectation values (vev) v_S and v , the physical components from S and H can be written as $(v_S + s)/\sqrt{2}$ and $(v + h)/\sqrt{2}$, respectively. The non-zero v_S will induce a non-zero Z' mass given by: $m_{Z'}^2 = b^2 g'^2 v_S^2$. A non-zero v_S together with the non-zero v will induce mixing between s and h with the mixing parameter proportional to $\lambda_{SH} v v_S$. This mixing will change the masses m_s and m_h of s and h in the limit of without mixing. Since we will require $m_{Z'}$ to be much larger than the Z mass, this implies that m_s is also much larger than m_h . The mixing will reduce the usual Higgs mass m_h . However, since the parameter λ_{SH} is not fixed, if it is small enough the reduction in Higgs mass can be neglected. In any case, the effects of the mixing and also other term in the Higgs potential involving S and H will not affect our discussions in the following. We will not discuss them further here.

The relic density of the dark matter is controlled by annihilation of $\bar{\psi}\psi \rightarrow Z'^* \rightarrow l_i \bar{l}_i + \nu_i \bar{\nu}_i$. The annihilation rate of dark matter σv , with lepton masses neglected and summed over the two types of charged leptons and neutrinos, is given by

$$\sigma v = \frac{3}{\pi} \frac{a^2 g'^4 m_\psi^2}{(s - m_{Z'}^2)^2 + \Gamma_{Z'}^2 m_{Z'}^2}, \quad (3)$$

where v is the relative velocity of the two annihilating dark matter and s is the total dark matter pair energy squared in the center of mass frame. $\Gamma_{Z'}$ is the decay width of the Z' boson. If the Z' mass is below the $\bar{\psi}\psi$ threshold which we will assume, the dominant decay modes of Z' are $Z' \rightarrow \bar{l}_i l_i + \bar{\nu}_i \nu_i$, and $\Gamma_{Z'}$ is given by, neglecting lepton masses

$$\Gamma_{Z'} = \frac{3g'^2}{12\pi} m_{Z'} . \quad (4)$$

In Eqs. (3) and (4), we have assumed that there are only left-handed light neutrinos. If there are light right-handed neutrinos to pair up with left-handed neutrinos to form Dirac neutrinos, the factor 3 in these equations should be changed to 4.

III. THE BREIT-WIGNER ENHANCEMENT AND BOOST FACTOR

Since the relic density of DM is determined by the annihilation rate, the model parameters are thus constrained. The same parameters will also determine the annihilation rate producing the electron/positron excess observed today, which requires a much larger annihilation rate. A boost factor in the range 100 to 1000 is necessary. We find that Breit-Wigner resonance enhancement mechanism works very well in our models if the Z' boson mass is about two times of the dark matter mass.

The boost factor in this case comes from the fact that since the Z' mass $m_{Z'}$ is close to two times of the dark matter mass m_ψ , the annihilate rate is close to the resonant point and is very sensitive to the thermal kinetic energy of dark matter. To see this let us rewrite the annihilation rate into a pair of charged leptons as

$$\sigma v = \frac{a^2 g'^4}{16\pi m_\psi^2} \frac{1}{(\delta + v^2/4)^2 + \gamma^2} , \quad (5)$$

where we have used the non-relativistic limit of $s = 4m_\psi^2 + m_\psi^2 v^2$, with δ and γ defined as $m_{Z'}^2 = 4m_\psi^2(1 - \delta)$, and $\gamma^2 = \Gamma_{Z'}^2(1 - \delta)/4m_\psi^2$.

For thermal dark matter, the velocity v^2 is proportional to the thermal energy of dark matter. It is clear that for small enough δ and γ , the annihilation rate is very sensitive to the thermal energy and therefore the thermal temperature T . At lower dark matter thermal energies, the annihilation rate is enhanced compared with that at higher temperature. This results in a very different picture of dark matter annihilation than the case for the usual non-resonant annihilation where the annihilation rate is not sensitive to dark matter thermal

energies. The annihilation process does not freeze out even after the usual “freeze out” time in the non-resonant annihilation case due to the enhanced annihilation rate at lower energies. To produce the observed dark matter relic density, the annihilation rate at zero temperature is required to be larger than the usual one, and therefore a boost factor. With appropriate δ and γ , a large enough boost factor can be produced.

For a detailed discussion, a precise form for the thermally averaged annihilation rate should be used which can be written as[24]

$$\langle\sigma v\rangle = \frac{1}{n_{EQ}^2} \frac{m_\psi}{64\pi^4 x} \int_{4m_\psi^2}^{\infty} \hat{\sigma}(s) \sqrt{s} K_1\left(\frac{x\sqrt{s}}{m_\psi}\right) ds, \quad (6)$$

with

$$n_{EQ} = \frac{g_i}{2\pi^2} \frac{m_\psi^3}{x} K_2(x), \quad (7)$$

$$\hat{\sigma}(s) = 2g_i^2 m_\psi \sqrt{s - 4m_\psi^2} \cdot \sigma v, \quad (8)$$

where g_i is the internal degrees of freedom of DM particle which is equal to 4 for a vector fermion, $K_1(x)$ and $K_2(x)$ are the modified Bessel functions of the second type.

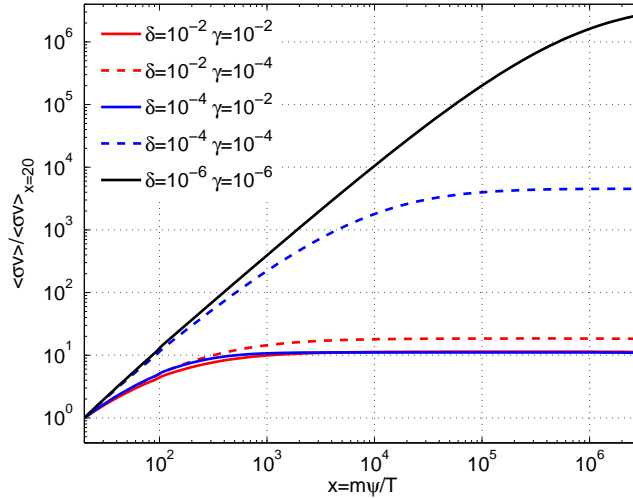


FIG. 1: The Breit-Wigner enhanced relative cross section $\langle\sigma v\rangle/\langle\sigma v\rangle_{x=20}$ as a function of time x .

We plot in Fig. 1 the thermally averaged annihilation rate $\langle\sigma v\rangle$ as a function of cosmic time $x \equiv m_\psi/T$ for several values of parameters γ and δ . The annihilation rate when “freeze out” at $x \approx 20$ is adopted as a normalization to illustrate the enhancement effect today.

To precisely determine the parameters we solve the standard Boltzmann equation of the decoupling process numerically. Fig. 2 shows an example of the evolution of DM abundance

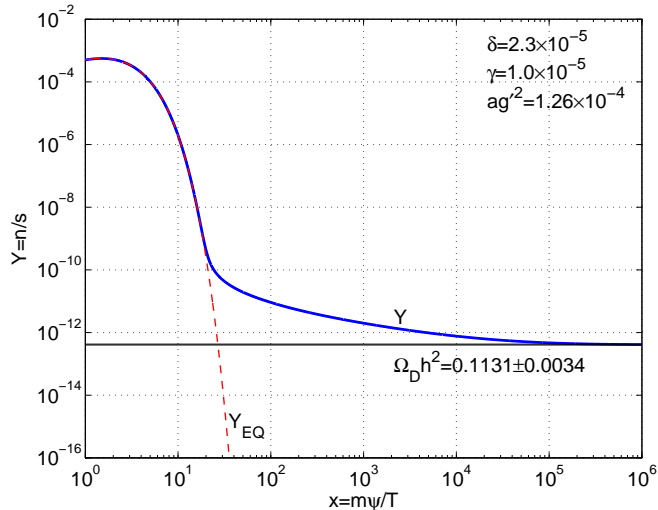


FIG. 2: The evolution of DM abundance Y as a function of x , compared with the equilibrium abundance $Y_{EQ} \propto x^{3/2}e^{-x}$ and the experimental measurements $\Omega_D h^2 = 0.1131 \pm 0.0034$ [27].

$Y = n/s$ with n and s the number density and entropy density respectively. The parameter ag^2 is adjusted to make sure that today's DM abundance is correct $Y(x = 3 \times 10^6) = Y_0 \equiv \Omega_D h^2 / 2.8 \times 10^8 (m_\psi / \text{GeV})$.

IV. THE ELECTRON/POSITRON SPECTRUM

We now discuss the DM annihilation produced electron/positron spectrum in the $U_{L_i-L_j}$ DM models for all the three possibilities discussed before: a) $L_e - L_\mu$; b) $L_e - L_\tau$; and c) $L_\mu - L_\tau$. In all these cases, 2/3 of the DM annihilate into charged lepton pairs and 1/3 into neutrino pairs, therefore the required boost factor should be 1.5 times of the case for DM only annihilate into charged lepton pairs.

After the electron/positron pairs produced by DM annihilation they propagate diffusively in the Galaxy due to the scattering with random magnetic field [28]. The propagation processes in the Galaxy is calculated numerically in order to compare with data measured at the Earth. The interactions with interstellar medium, mainly the synchrotron radiation and inverse Compton scattering processes, will lead to energy losses of the primary electrons and positrons. In addition, the overall convection driven by the Galactic wind and reacceleration due to the interstellar shock will also affect the electron spectrum. In this work we solve the propagation equation numerically adopting the GALPROP package [29].

In Fig. 3 we show the model predictions on the $e^+/(e^+ + e^-)$ fraction and $e^+ + e^-$ fluxes together with the observational data. The background is also calculated using GALPROP package [29] with the diffusion + convection model parameters developed in Ref. [17]. Following Ref. [30], to fit ATIC and PAMELA data we adopt the DM mass ~ 1 TeV and Merritt density profile. In addition for the $U(1)_{L_\mu-L_\tau}$ (model c) we also plot the spectrum with DM mass 1.5 TeV to fit the Fermi result. A boost factor ~ 1200 (we have included the branching ratio into neutrinos which do not produce electron/positron excess)¹, or equivalently $\langle\sigma v\rangle \approx 3.6 \times 10^{-23} \text{ cm}^3 \text{ s}^{-1}$, is found to give good description to the data [30] (The cross section for 1.5TeV DM to fit Fermi requires the a slightly larger value of $\sim 5.4 \times 10^{-23} \text{ cm}^3 \text{ s}^{-1}$). Considering the errorbars of the ATIC data, we find that $\langle\sigma v\rangle = 2.7 - 4.5 \times 10^{-23} \text{ cm}^3 \text{ s}^{-1}$ (corresponding to a boost factor 900–1500) can be consistent with the observations.

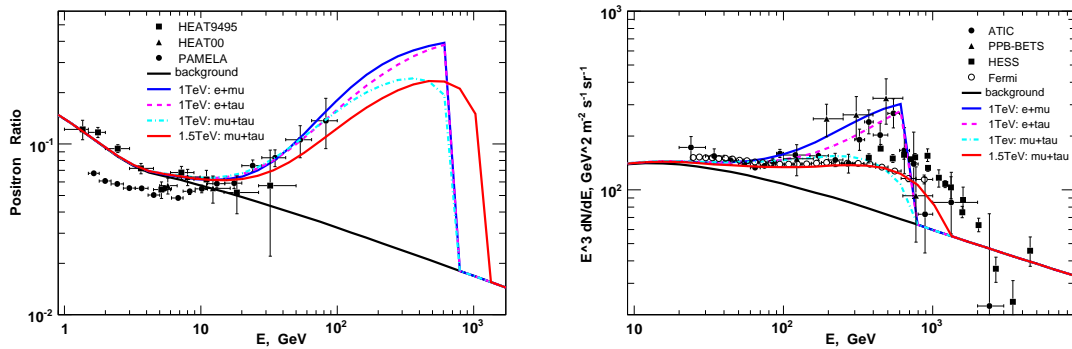


FIG. 3: *Left:* positron fraction $e^+/(e^+ + e^-)$ predicted in the $U(1)_{L_i-L_j}$ model compared with the observational data from PAMELA [3] and HEAT [5, 31]. *Right:* the total electron spectrum of the model, compared with observations of ATIC [1], PPB-BETS [2], Fermi [8] and H.E.S.S. [32].

For our model scenarios, in the cases a) and b) one of the pairs is directly annihilated into electron/positron pair and another pair with secondary electron/positron pair. As can be seen from Fig. 3, these two cases predict a sharp falling of electron/positron in the spectrum at energy about 600 GeV and fit the ATIC data very well. We also note that the case b) is slightly favored over case a), but the difference is very small.

For the case c), the electron/positron pairs come from secondary decay of muon pair and tauon pairs. If one normalizes the boost factor to PAMELA data, there is no sharp falling in

¹ Note that the boost factor in Ref. [30] is defined as $\langle\sigma v\rangle/3 \times 10^{26} \text{ cm}^3 \text{ s}^{-1}$, instead of the one $\langle\sigma v\rangle/\langle\sigma v\rangle_{x=20}$ as shown in Fig. 1.

the electron/positron spectrum at around 600GeV. This model cannot fit ATIC data well. Since this model has a softer spectrum, one wonders whether it can fit Fermi data. It is clear from Fig. 3 that for DM mass of ~ 1 TeV it can not fit the Fermi data either. However, we see from Fig. 3 that with a 1.5 TeV DM mass the soft electron spectrum can fit the Fermi data very well, and at the same time it can also account for the PAMELA data of positron ratio.

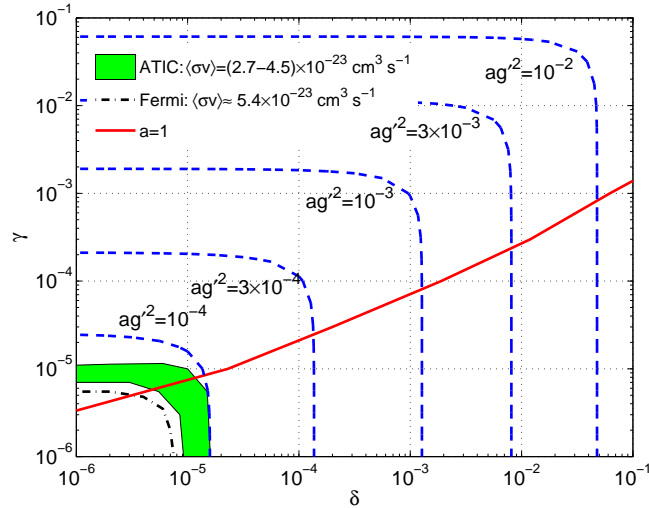


FIG. 4: Constraints on the model parameters from the DM relic density and the cosmic ray data on the $\gamma - \delta$ plane. Dashed lines show the isolines with ag'^2 adjusted to satisfy the DM relic density. Shaded region shows the allowed parameter ranges with additional PAMELA/ATIC constraints, while the dot-dashed line shows the constraint from the best fitting cross section for PAMELA/Fermi data. The $a = 1$ curve is given by requiring correct relic density.

Finally combining the constraints on the model parameters from the relic density and PAMELA, ATIC/Fermi data we can derive the model parameters, which are shown in Fig. 4. By properly adjusting the ag'^2 , the whole parameter space of $\gamma - \delta$ can give the right relic density. However, to give the needed boost factor which can account for the cosmic ray electron/positron data, the parameters are further limited in a much narrower range, as shown by the shaded region in Fig. 4, which gives a fit to the PAMELA/ATIC data. For the model to fit PAMELA/Fermi data, we need a heavier DM mass and a bit larger cross section. The constraint is shown by the dot-dashed curve in Fig. 4. We did not take the errors of Fermi data into account since they have very small statistic errors. We also plot

an $a = 1$ curve which gives correct relic density while setting $a = 1$. The overlap between the $a = 1$ curve with the shaded region gives the correct relic density and boost factor to account for ATIC and PAMELA data with universal gauge couplings between dark matter and SM leptons. The allowed range of g' with $a = 1$ is $6.5 \times 10^{-5} \lesssim g'^2 \lesssim 9.2 \times 10^{-5}$. Then we have $5.5 \times 10^{-6} \lesssim \gamma \lesssim 7.5 \times 10^{-6}$ and $5 \times 10^{-6} \lesssim \delta \lesssim 1.2 \times 10^{-5}$ for $a = 1$ to give correct relic density and boost factor. Similarly for the model to fit PAMELA/Fermi data we have $g'^2 \approx 5.8 \times 10^{-5}$, $\gamma \approx 4.8 \times 10^{-6}$ and $\delta \approx 3.5 \times 10^{-6}$. In principle there should also be a narrow range satisfy the experimental constraints, which are not shown here. For $a \neq 1$ case, one can extract a and g'^2 separately from Fig. 3 by the fact $\gamma \approx 3g'^2/12\pi$ in our models with a known ag'^2 . An interesting thing to note is that the Y' charge of the dark matter does not need to be very different from the SM leptons.

V. DISCUSSIONS AND CONCLUSIONS

In this paper we studied a class of leptophilic dark matter model with $U(1)_{L_i-L_j}$ gauge interactions to account for the recent cosmic ray results. We have shown that two of the anomaly free gauged $U(1)_{L_i-L_j}$ models, the gauged $U(1)_{L_e-L_\mu}$ and $U(1)_{L_e-L_\tau}$ models, can naturally explain the excess in electron/positron spectrum at ATIC, while another model with $U(1)_{L_\mu-L_\tau}$ gauge coupling can naturally account for the electron spectrum at Fermi. We have seen that in order to fit data the regions allowed for g'^2 and a are constrained to narrow regions. Plus the facts that the dark matter is required to be about 1 TeV to explain the sharp falling in electron/positron excess at ATIC or about 1.5 TeV to best fit the Fermi and HESS data, and Z' mass is required to be about two times of the dark matter mass to have a large boost factor via the Breit-Wigner enhancement mechanism, the models parameters are all determined in narrow regions.

Since the model parameters are restricted to narrow regions, one has to check if the constraints on the models are compatible with other processes. A closely related process is direct dark matter search. The annihilation process, $\psi + \bar{\psi} \rightarrow e^+ + e^-$, producing the relic dark matter density and the electron/positron excess, is related to the direct detection process by changing the interaction from s-channel to t-channel, i.e., $\psi + e \rightarrow \psi + e$. One may worry if the enhanced s-channel cross section, a large boost factor, will also lead to a large t-channel cross section resulting in conflict with direct detection results. This is not

the case.

For $\psi + e \rightarrow \psi + e$ collision with ψ mass of around 1 TeV (or 1.5 TeV), the energy transferred to the electron is very small, at the eV order, far below the threshold energy of present detectors. However, if the dark matter particle ψ kicks out a tightly bound electron, the energy transferred to the electron may be larger and detectable. But even this happens, the interaction cross section for the t-channel is still too small because in this case there is no Breit-Wigner enhancement, $\sigma(\psi + e \rightarrow \psi + e) = (6a^2 g'^2 / \pi) m_e^{*2} / m_{Z'}^4$. Here m_e^* indicates a free electron or a tightly bound electron. Using the bounds on the model parameters obtained before, we find that the cross section is of order $(m_e^{*2} / \text{GeV}^2) \times 10^{-48} \text{cm}^2 (2\text{TeV} / m_{Z'})^2$, which is well below the sensitivities of the present detectors.

Low energy processes such as g-2 of electron, muon or tauon, $e - \nu$ collision data, and also high energy experiments at LEP have put stringent constraints on possible electron interaction with new gauge particles. However, in contributions from Z' are all proportional to $g'^2 / m_{Z'}^2$, which is of order $10^{-11} / a(\text{GeV}^{-2})(2\text{TeV} / m_{Z'})^2$. If a is of order one there is no conflict with data.

Direct production of Z' will be very difficult at LHC since at tree level the Z' only interacts directly with electron, muon/tauon. ILC will not be able to produce directly Z' either since its energy is below the Z' mass. But Z' can be produced at CLIC for models a) and b) where the e^+e^- center of mass frame energy can be as high as 3 TeV. It may be interesting to scan the machine energy around the Z' resonant region to discover it. The decay widths of Z' in models considered here are of order 10 MeV. This requires a very careful scanning. For model c), a muon collider may provide a chance to produce the relevant Z' boson.

Finally we point out that our study can be easily extended to a larger group of dark matter models that are leptophilic. Once we assume the Breit-Wigner enhancement takes effect to explain both the relic density and positron excess today the model parameters can be determined within a quite definite range, which should be similar to the present results.

In summary, in the present work we have constructed simple dark matter models with gauged $U(1)_{L_i-L_j}$ interactions. We have shown that the direct electron component in the annihilation final states are necessary to account for the sharp falling at the ATIC electron spectrum at $\sim 600\text{GeV}$. The $U(1)_{L_e-L_\mu}$ and $U(1)_{L_e-L_\tau}$ models with the dark matter mass around 1 TeV are in excellent agreement with ATIC data. However, to explain Fermi data which does not show the sharp falling indicated by ATIC data, one should avoid having

direct electron component. This fact favors $U(1)_{L_\mu-L_\tau}$ model. All these models predict quite definite coupling constant, Z' mass and width, which are consistent with all present collider and other low energy data.

At present ATIC or Fermi data is consistent with PAMELA data separately, but ATIC and Fermi data do not agree with each other. Although one can find models which fit one of the two data sets, i) PAMELA and ATIC, and ii) PAMELA and Fermi, it is obvious that these models cannot simultaneously all be correct. To finally decide which DM model is correct, experimental data have to give an unique set of data which can only be achieved by future improved experiments. Only by then one can decide the correct dark matter model.

Acknowledgments

We thank Wanlei Guo and Henry Wong for useful discussions and Juan Zhang for help plotting one figure. This work was supported in part by the NSF of China under grant No. 10773011, by the Chinese Academy of Sciences under the grant No. KJCX3-SYW-N2, by NSC and NCTS.

-
- [1] J. Chang *et al.*, Nature **456**, 362 (2008).
 - [2] S. Torii *et al.*, arXiv:0809.0760 [astro-ph].
 - [3] O. Adriani *et al.*, arXiv:0810.4995 [astro-ph].
 - [4] O. Adriani *et al.*, arXiv:0810.4994 [astro-ph].
 - [5] S. W. Barwick *et al.* [HEAT Collaboration], Astrophys. J. **482**, L191 (1997).
[arXiv:astro-ph/9703192].
 - [6] M. Aguilar *et al.* [AMS-01 Collaboration], Phys. Lett. B **646**, 145 (2007).
[arXiv:astro-ph/0703154].
 - [7] J. Chang, W.K.H. Schmidt, J.H. Adams *et al.*, Proc. of 29th ICRC (Pune) 3, 1-4, 2005.
 - [8] Fermi/LAT Collaboration, arXiv:0905.0025v1 [astro-ph.HE].
 - [9] D. Hooper, P. Blasi and P. D. Serpico, arXiv:0810.1527 [astro-ph].
 - [10] H. Yuksel, M. D. Kistler and T. Stanev, arXiv:0810.2784 [astro-ph].
 - [11] S. Profumo, arXiv:0812.4457 [astro-ph].

- [12] H. B. Hu, Q. Yuan, B. Wang, C. Fan, J. L. Zhang and X. J. Bi, arXiv:0901.1520 [astro-ph].
- [13] L. Bergstrom, T. Bringmann and J. Edsjo, arXiv:0808.3725 [astro-ph]; M. Cirelli and A. Strumia, arXiv:0808.3867 [astro-ph]; V. Barger, W. Y. Keung, D. Marfatia and G. Shaughnessy, arXiv:0809.0162 [hep-ph]; J. H. Huh, J. E. Kim and B. Kyae, arXiv:0809.2601 [hep-ph]; C. R. Chen and F. Takahashi, arXiv:0810.4110 [hep-ph]; A. E. Nelson and C. Spitzer, arXiv:0810.5167 [hep-ph]; I. Cholis, D. P. Finkbeiner, L. Goodenough and N. Weiner, arXiv:0810.5344 [astro-ph]; Y. Nomura and J. Thaler, arXiv:0810.5397 [hep-ph]; D. Feldman, Z. Liu and P. Nath, arXiv:0810.5762 [hep-ph]; K. Ishiwata, S. Matsumoto and T. Moroi, arXiv:0811.0250 [hep-ph]; Y. Bai, Z. Han, arXiv:0811.0387v1 [hep-ph]; C. R. Chen, F. Takahashi and T. T. Yanagida, arXiv:0811.0477 [hep-ph]; K. Hamaguchi, E. Nakamura, S. Shirai and T. T. Yanagida, arXiv:0811.0737 [hep-ph]; E. Ponton and L. Randall, arXiv:0811.1029 [hep-ph]; A. Ibarra and D. Tran, arXiv:0811.1555 [hep-ph]; C. R. Chen, F. Takahashi and T. T. Yanagida, arXiv:0811.3357 [astro-ph]; I. Cholis, G. Dobler, D. P. Finkbeiner, L. Goodenough and N. Weiner, arXiv:0811.3641 [astro-ph]; E. Nardi, F. Sannino and A. Strumia, arXiv:0811.4153 [hep-ph]; E. J. Chun and J. C. Park, arXiv:0812.0308 [hep-ph]; J. Liu, P. F. Yin and S. H. Zhu, arXiv:0812.0964 [astro-ph]; R. Allahverdi, B. Dutta, K. Richardson-McDaniel and Y. Santoso, arXiv:0812.2196 [hep-ph]; K. Hamaguchi, S. Shirai and T. T. Yanagida, arXiv:0812.2374 [hep-ph]; D. Hooper, A. Stebbins and K. M. Zurek, arXiv:0812.3202 [hep-ph]; K. J. Bae, J. H. Huh, J. E. Kim, B. Kyae and R. D. Viollier, arXiv:0812.3511 [hep-ph]; S. Khalil, H. S. Lee and E. Ma, arXiv:0901.0981 [hep-ph]; X.-J. Bi, P.-H. Gu, T.-J. Li, X.-M. Zhang, arXiv:0901.0176 [hep-ph]; S. C. Park, J. Shu, arXiv:0901.0720v1 [hep-ph]; Q. H. Cao, E. Ma and G. Shaughnessy, arXiv:0901.1334 [hep-ph]; F. Takahashi and E. Komatsu, arXiv:0901.1915 [astro-ph]; C. H. Chen, C. Q. Geng and D. V. Zhuridov, arXiv:0901.2681 [hep-ph]; P. Meade, M. Papucci and T. Volansky, arXiv:0901.2925 [hep-ph]; J. Mardon, Y. Nomura, D. Stolarski and J. Thaler, arXiv:0901.2926 [hep-ph]; X. Chen, arXiv:0902.0008 [hep-ph]; B. Kyae, arXiv:0902.0071 [hep-ph]; D. Hooper and K. Zurek, arXiv:0902.0593 [hep-ph]; Hock-Seng Goh, Lawrence J. Hall, Piyush Kumar, arXiv:0902.0814v2 [hep-ph]; R. Allahverdi, B. Dutta, K. Richardson-McDaniel, Y. Santoso, arXiv:0902.3463; K. J. Bae and B. Kyae, arXiv:0902.3578 [hep-ph]; K. Cheung, P. Y. Tseng and T. C. Yuan, arXiv:0902.4035 [hep-ph].
- [14] M. Cirelli, M. Kadastik, M. Raidal and A. Strumia, arXiv:0809.2409 [hep-ph].

- [15] N. Arkani-Hamed, D. P. Finkbeiner, T. Slatyer and N. Weiner, arXiv:0810.0713 [hep-ph].
- [16] M. Pospelov and A. Ritz, arXiv:0810.1502 [hep-ph]; F. Chen, J. M. Cline and A. R. Frey, arXiv:0901.4327 [hep-ph].
- [17] P. F. Yin, Q. Yuan, J. Liu, J. Zhang, X. J. Bi, S. H. Zhu and X. M. Zhang, arXiv:0811.0176 [hep-ph].
- [18] P. J. Fox and E. Poppitz, arXiv:0811.0399 [hep-ph].
- [19] S. Baek, P. Ko, arXiv:0811.1646 [hep-ph].
- [20] L. Bergstrom, J. Edsjo, G. Zaharijas, arXiv:0905.0333v1 [astro-ph.HE]; D. Grasso et al., arXiv:0905.0636 [astro-ph.HE].
- [21] X. G. He, G. C. Joshi, H. Lew and R. R. Volkas, Phys. Rev. D **43** (1991) 22; X. G. He, G. C. Joshi, H. Lew and R. R. Volkas, Phys. Rev. D **44** (1991) 2118; R. Foot, X. G. He, H. Lew and R. R. Volkas, Phys. Rev. D **50** (1994) 4571 [arXiv:hep-ph/9401250]; S. Baek, N. G. Deshpande, X. G. He and P. Ko, Phys. Rev. D **64** (2001) 055006 [arXiv:hep-ph/0104141]; E. Ma, D. P. Roy and S. Roy, Phys. Lett. B **525**, 101 (2002) [arXiv:hep-ph/0110146].
- [22] W.B. Lin, D.H. Huang, X. Zhang, R.H. Brandenberger, Phys. Rev. Lett. **86**, 954 (2001); R. Jeannerot, X. Zhang and R. Brandenberger, JHEP 9912, 003 (1999).
- [23] J. Hisano, S. Matsumoto, M. M. Nojiri and O. Saito, Phys. Rev. D **71**, 063528 (2005) [arXiv:hep-ph/0412403]. J. Hisano, S. Matsumoto, M. Nagai, O. Saito and M. Senami, Phys. Lett. B **646**, 34 (2007) [arXiv:hep-ph/0610249]. M. Cirelli, A. Strumia and M. Tamburini, Nucl. Phys. B **787**, 152 (2007) [arXiv:0706.4071 [hep-ph]]. M. Lattanzi and J. I. Silk, arXiv:0812.0360 [astro-ph].
- [24] M. Ibe, H. Murayama and T. T. Yanagida, arXiv:0812.0072 [hep-ph]; W. L. Guo and Y. L. Wu, arXiv:0901.1450 [hep-ph].
- [25] J. Lavalle, Q. Yuan, D. Maurin and X. J. Bi, Astron. Astrophys. **479**, 427 (2008). [arXiv:0709.3634 [astro-ph]].
- [26] J. Lavalle, E. Nezri, F. S. Ling, L. Athanassoula and R. Teyssier, arXiv:0808.0332 [astro-ph].
- [27] E. Komatsu *et al.* [WMAP Collaboration], Astrophys. J. Suppl. **180**, 330 (2009) [arXiv:0803.0547 [astro-ph]].
- [28] T.K. Gaisser, *Cambridge, UK: Univ. Pr. (1990) 279 p*
- [29] A. W. Strong and I. V. Moskalenko, Astrophys. J. **509**, 212 (1998). [arXiv:astro-ph/9807150]. I. V. Moskalenko and A. W. Strong, Astrophys. J. **493**, 694 (1998). [arXiv:astro-ph/9710124].

- [30] J. Zhang, X. J. Bi, J. Liu, S. M. Liu, P. f. Yin, Q. Yuan and S. H. Zhu, arXiv:0812.0522 [astro-ph].
- [31] S. Coutu *et al.*, in *Proceedings of the 27th International Cosmic Ray Conference* (Hamburg, 2001), Vol. 5, p. 1687.
- [32] H. E. S. S. Collaboration, *Phys. Rev. Lett.* **101**, 261104 (2008).